Polyostotic hyperostosis in a domestic shorthair cat

Anne Fawcett, Richard Malik, C Rolfe Howlett, Michelle M McDonald, John Culvenor, Roy Pool and Graeme S Allan

Journal of Feline Medicine and Surgery 2014 16: 432
DOI: 10.1177/1098612X14530216

Journal of Feline Medicine and Surgery (2014) **16**, 432–440

CASE REPORT

Polyostotic hyperostosis in a domestic shorthair cat

Anne Fawcett
BA(Hons) BSc(Vet)(Hons) BVSc(Hons) MVetStud[1,2]

Richard Malik
DVSc DipVetAn MVetClinStud PhD FACVSc FASM[3]

C Rolfe Howlett
BVSc PhD MACVSc FBSE[4]

Michelle M McDonald
BMedSci PhD[5]

John Culvenor
BVSc MVSt FACVSc[6]

Roy Pool
DVM PhD[7]

Graeme S Allan
MVSc FACVSc DipACVR DVSc[8]

[1]Sydney Animal Hospitals – Inner West, 1a Northumberland Avenue, Stanmore, NSW 2048, Australia
[2]Faculty of Veterinary Science, University of Sydney, Camperdown, NSW 2006, Australia
[3]Centre of Veterinary Education, B22 University of Sydney, Camperdown, NSW 2006, Australia
[4]Vetnostics, 60 Waterloo Road, North Ryde, NSW 2113, Australia
[5]Garvan Institute of Medical Research, Darlinghurst, NSW 2010, Australia
[6]North Shore Veterinary Specialist Centre, 64 Atchinson Street, Crows Nest, NSW 2065, Australia
[7]Department of Pathobiology, College of Veterinary Medicine and Biomedical Sciences, Texas A&M University, College Station, TX 7784, USA
[8]Veterinary Imaging Associates, St Leonards, NSW 1590, Australia

Corresponding author:
Anne Fawcett,
fawcettanne@gmail.com

Date accepted:
17 February 2014

Clinical presentation: An 11-year-old male neutered domestic shorthair cat was presented for investigation of weight loss and inappetence. On physical examination there was palpable enlargement and thickening of many bones, and this finding was confirmed radiographically.

Proposed diagnosis: Based on clinical, radiological and histopathological findings, a polyostotic bone disease, best described as generalised idiopathic hyperostosis, was diagnosed. This condition has not been reported in cats previously. Canine and human diseases with similarities to this presentation are discussed.

Clinical report

An 11-year-old male neutered domestic shorthair cat (3.0 kg) was presented with inappetence and weight loss. It had been adopted in Japan as a stray with two presumed littermates, all found together in a cardboard box, when the litter was approximately 8 weeks of age. At 3 years old an elevation of one of the cat's liver enzymes (not specified in the history) was detected during a routine health screen. The cat was fed Hill's l/d for 2 years subsequently, but the owners could not recall whether the diet was discontinued due to normalisation of liver enzyme activity or for convenience.

One of the littermates was euthanased due to advanced chronic kidney disease at approximately 9 years of age. The owners relocated to Australia in 2007 with the remaining two cats, then 9 years old.

On arrival, a veterinarian for the Australian Quarantine Inspection Service noted that this particular cat had 'deformed front legs, swollen back legs' and was 'very thin'. However, the officer was unable to perform a complete physical examination due to the cat's fractious nature.

The owners reported that the cat appeared to have had lifelong valgus deformity of both carpi and had never jumped up higher than 30 cm. The cat had a history of chronic constipation (untreated) and, more recently, dysphagia, specifically difficulty prehending dry food. Both cats lived strictly indoors and both ate dry urinary s/o (Royal Canin) and canned Hill's c/d diet, presumably due to a urinary tract condition of one or both cats which was not explained in the case notes from overseas. Vaccinations were current and there was no history of trauma.

Figure 1 The cat on presentation. Note the marked carpal valgus and plantigrade hindlimb stance

Physical examination

The cat was alert and responsive on presentation. Physical examination was difficult due to the cat's aggressive behaviour. It was thin (body condition score 2/5). Palpation revealed extensive thickening of

DOI: 10.1177/1098612X14530216

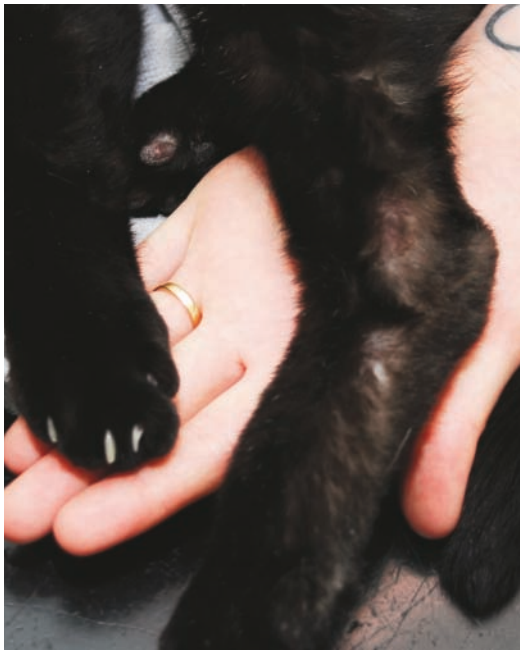

Figure 2 Marked thickening of the hock with fur loss over bony prominences

the mandible and long bones. Range of motion of the proximal appendicular joints was markedly reduced. There was pronounced carpal valgus (Figure 1) and marked thickening of the hocks (Figure 2). Abdominal palpation revealed a large column of hard faeces in the colon. All paw pads had a peeling epithelial surface (Figure 3). The cat was mildly hypothermic (rectal temperature 36.7°C).

The patient was considered to have generalised skeletal disease, most likely due to an inborn error of bone metabolism. At that time our conclusions were that the history was not consistent with hypervitaminosis A and other

Figure 4 Ventrodorsal radiograph of the head demonstrating thickened mandibular rami

Figure 3 Close-up of the paw pads, showing the peeling epithelial surface

diagnostic possibilities included acromegaly, generalised osteomyelitis, osteopetrosis or a disorder of calcium metabolism.

Laboratory testing

A complete blood count revealed a mild neutrophilia (16.4 x 10^9/l; reference interval [RI] 2–13 x 10^9/l) and marginal monocytosis (0.8 x 10^9/l; RI <0.7 x 10^9/l). Serum biochemical abnormalities included hypernatraemia (164 mmol/l; RI 144–158 mmol/l), hyperchloraemia (125 mmol/l; RI 106–123 mmol/l), increased urea (26.4 mmol/l; RI 5–15 mmol/l) consistent with dehydration and likely pre-renal azotaemia, and increased alkaline phosphatase (51 mmol/l; RI 5–10 mmol/l) concentrations. Total thyroxine concentration was unremarkable (13 nmol/l; RI 10–61 nmol/l). Urinalysis revealed reduced concentrating ability (urine specific gravity 1.028), mild proteinuria (1+) and marked haematuria (4+). Based on failure to adequately concentrate urine in the face of dehydration, a diagnosis of chronic kidney disease (IRIS stage 1A) was made.

The serum parathyroid hormone concentration (28.6 pg/ml; RI 22–168 pg/ml), 25-hydroxy-vitamin D_3 concentration (106 nmol/l; RI 88–168) and insulin-like growth factor-1 (395 µg/l; RI <800 µg/l) were all normal. Serology for leishmaniasis (Kalazar ELISA), ehrlichiosis (Ehrlichia canis IFA) and anaplasmosis (complement fixation test) were all negative. In-house serology for feline immunodeficiency virus (FIV) antibodies and feline leukaemia virus (FeLV) antigen (Anigen Rapid FIV Ab/FeLV Ag Test Kit, Bionote) was negative.

Diagnostic imaging

Radiographs of the appendicular and axial skeleton were obtained under general anaesthesia. A notable radiographic feature of the images taken in March 2009 included bilaterally symmetrical uniform thickening of the mandibular rami (Figure 4) (thickness from

A notable radiographic feature was bilaterally symmetrical uniform thickening of the mandibular rami.

Figure 5 Lateral radiograph of the skull and cervical spine. Note the thickened skull and mandibles and the coarse trabecular pattern in the vertebrae

Figure 6 Mediolateral view of the left forelimb. The humerus, radius, ulna and metacarpals all demonstrate hyperostosis

the axial to abaxial surface of the rami was 19 mm [left] and 20 mm [right]). The mandibular bone was smoothly marginated with homogeneous radiopacity. There was no evidence of cancellous bone in either mandibular ramus, all bone appearing to be cortical in morphology. In the skull the frontal bone and the calvarium were uniformly thickened (5 mm and 6 mm, respectively) (Figure 5).

In the forelimbs the humeri, radii, ulnae, metacarpals and phalanges of the manus were all affected in a similar manner, except that a narrow medulla was present in affected bones of the appendicular skeleton. The humeri measured 24 mm and 26 mm diameter, and the paired bones of the antebrachii measured 24 mm and 28 mm diameter (Table 1). Increase in diaphyseal bone volume appeared to be cortical in origin and expansion appeared both concentric and eccentric, with florid new bone being laid down on both the periosteal and endosteal surfaces of long bone diaphyses (Figure 6). Similar changes affected the femurs, tibiae, fibulae, metatarsal bones and phalanges of the pes (Figure 7). The bones of the pelvis appeared wider than expected, with accentuation of trabeculae in the vertebrae and pelvis (Figure 8). The diarthrodial joints of the appendicular skeleton and the adjacent epiphyses appeared to be spared the proliferative changes in the long bones, although signs of degenerative remodelling were present in many joints, resulting in osteoarthritis. In the axial skeleton the ribs appeared wider than normal for a cat.

Figure 7 Lateral radiograph of the right stifle and hock. The femur, tibia, fibula, calcaneus and metatarsals have demonstrable hyperostosis

Figure 8 Ventrodorsal radiograph of the pelvis. A coarse trabecular pattern is visible in the pelvis

The cat's littermate was radiographed for comparison. There were no signs of increased bone thickening or opacity, trabecular thickening or degenerative joint disease, except for signs of ankylosing spondylopathy of the lower lumbar vertebrae, which was considered a normal finding for a cat of this age.

Table 1 Relative bone measurements of the affected cat and the unaffected littermate

	Mandible width	Frontal bone thickness	Calvarium thickness	Humeral diameter	Antebrachial diameter
Affected cat	L19 mm, R20 mm	5 mm	6 mm	L24 mm, R26 mm	L24 mm, R28 mm
Unaffected cat	L5 mm, R5 mm	2 mm	3 mm	L11 mm, R11 mm	L15 mm, R15 mm

Sonographic examination of the abdomen by an imaging specialist (GSA) revealed a striated pattern in the renal cortices, with recognisable corticomedullary architecture. Foci of mineralisation were evident in the renal parenchyma, with overall renal dimensions in the sagittal plane measuring 19–20 mm x 34–36 mm. No other sonographic abnormalities were detected in the abdomen. The appearance of the renal parenchyma was considered consistent with chronic interstitial nephritis.

Assessment and management

The skeletal changes appeared to be long-standing and, although severe, seemed unlikely to account for the cat's presenting complaints, which were considered referable to bacterial urinary tract infection secondary to inadequately concentrated urine. Regrettably this was not confirmed by microscopy and culture due to financial constraints.

The cat was admitted for intravenous fluid therapy (Hartmann's solution; 6 ml/kg/h for 24 h, then 3 ml/kg/h), antimicrobial therapy (amoxicillin–clavulanic acid, 20 mg/kg PO) and nutritional support (1 can Hill's a/d by syringe daily, divided into four meals). Following 3 days of intravenous fluid therapy, the cat was discharged on Ipakitine (Vetoquinol), a stool softener and inorganic phosphate binder. The cat continued to gain weight (at this point weighing 3.4 kg). Serial radiographs revealed no progression of skeletal changes.

Over the following 3 months the cat presented with two further episodes of haematuria, both of which were treated with an injectable antibiotic (cefovecin, 8 mg/kg SC) for presumptive urinary tract infections. When the haematuria did not resolve on the second occasion a urine culture was performed, revealing a heavy growth of *Escherichia coli* that was susceptible to cefovecin. A second injection was given 14 days after the first.

One year after initial radiographic assessment, the cat was re-radiographed under general anaesthesia (March 2010). The appearance of the mandibles, skull, vertebral column and appendicular skeleton was essentially unchanged. Measurements of the mandibular rami, humeri and antebrachii were similar to the measurements obtained 1 year earlier, suggesting that the bone condition was either non-progressive or slowly progressive. There were two new findings – an area of increased radiopacity in the dorsocaudal thorax, confluent with the crura of the diaphragm, and what appeared to be bilaterally symmetrical transverse fractures of both zygomatic arches. The thoracic opacity had the appearance of a neoplastic or inflammatory pulmonary nodule, while the zygomatic arch changes were most consistent with pathological fractures.

Fourteen months after the initial presentation, a bone biopsy was scheduled to further characterise the skeletal disorder. Repeat thoracic radiographs at this time failed to detect any radiographic signs of pulmonary disease.

At the time of writing, 4 years later, the owners report that, aside from intermittent urinary tract infections, treated successfully with antimicrobials, the cat remains bright and alert and has a normal appetite. However, the cat's mobility remains abnormal and limited, and body condition is suboptimal.

The skeletal changes appeared to be long-standing and, although severe, seemed unlikely to account for the cat's presenting complaints, which were considered referable to bacterial urinary tract infection.

Bone biopsy and labelling procedures

Oxytetracycline was used to label new bone deposition in order to determine bone turnover. Oxytetracycline was administered at a dose rate of 21 mg/kg PO at 12 h intervals, 17 and 16 days prior to bone biopsy, and again on days 5 and 4 prior to biopsy, to label new bone and thus permit an estimate of bone turnover.

The cat was premedicated with acepromazine (0.05 mg/kg) and butorphanol (0.2 mg/kg). Anaesthesia was induced with propofol, given to effect, and maintained using isoflurane in oxygen following endotracheal intubation. Intravenous fluids (Hartmann's solution) were administered perioperatively.

Following creation of dorsal skin incisions and elevation of the gluteal muscles, bone specimens were obtained from the crests of both iliac wings using a 15 mm diameter trephine. The ilia were 4–5 mm thick. The bone samples were placed in fixative. The cat recovered uneventfully from anaesthesia.

Histology and micromorphology of hyperostosis

Bone biopsies from both the affected cat and an unrelated normal cat were fixed in 4% paraformaldehyde for 3–4 days before being transferred to 70% ethanol. Biopsies were then scanned using a Skyscan MicroCT (μCT) at a resolution of 12 μm.

Upon completion of μCT analysis, the biopsies were decalcified for 8–10 weeks in 0.34 M EDTA at pH 8.0 before being processed to paraffin blocks. Samples were dehydrated in graded ethanols before being infiltrated with xylene and then embedded in paraffin wax. Sections were stained using haematoxylin/eosin and alcian blue/picrosirius red to assess bone morphology.[1] A tartrate-resistant acid phosphatase (TRAP) stain was used to assess osteoclast parameters. The second biopsy from the affected cat was processed to methylmethacrylate resin for undecalcified histology to assess bone formation through measuring interlabel distances between the serial oxytetracycline labels (Figure 9).

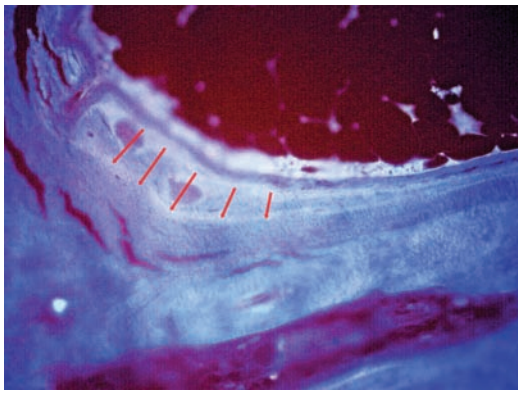

Figure 9 Image demonstrating the interlabel distance that was measured to generate mineral apposition rate. The red lines depict the distances measured between the two fluorescent labels (pale green) incorporated into the bone matrix (blue). Original magnification x 20

Analysis of the three-dimensional structure of both the trabecular and cortical compartment was performed on each biopsy within a 300 slice central region of interest, approximately 3.6 mm in diameter. Trabecular bone volume of total volume (BV/TV) was increased by 45% in the affected cat as compared with the control. Trabecular architecture was also considerably altered, with a 140% increase in trabecular thickness and a 40% reduction in trabecular number. These alterations in trabecular bone distribution are clearly appreciated in Figure 10. Cortical bone in the biopsies was also dramatically altered, both in volume and appearance, with 29% more cortical bone volume in the affected cat. This finding at the tissue level is consistent with the radiological findings of increased cortical thickening, along with increases in cancellous bone volume.

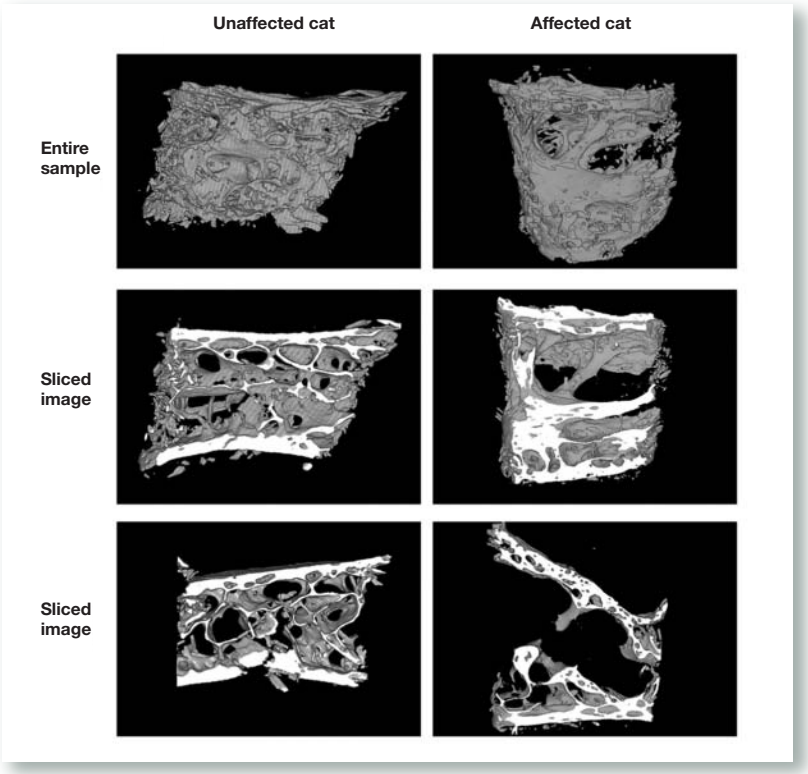

Figure 10 Images of the three-dimensional model of each biopsy generated from μCT scans. Note the loss of normal trabecular bone structure, greatly thickened trabeculae and reduced trabecular number in the affected cat compared with the unaffected cat

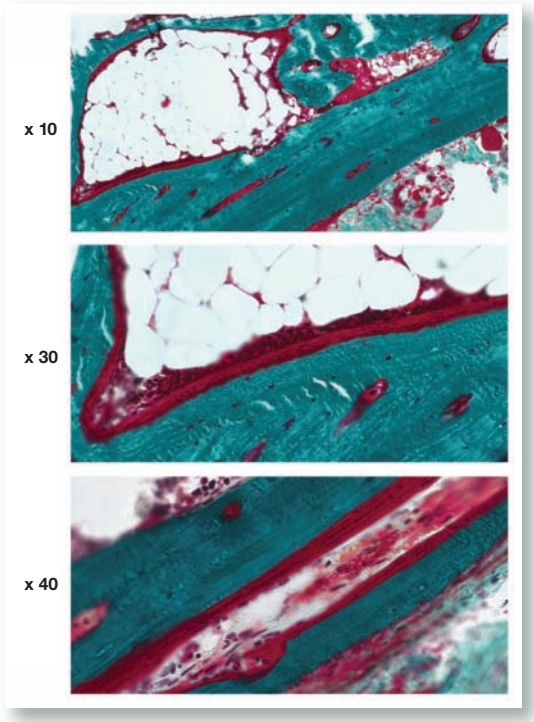

Figure 11 Representative images of undecalcified sections of bone from the affected cat. Sections are stained with Goldner's trichrome. Osteoid is red, mineralised bone matrix is green and nuclei are purple. Note the large amount of osteoid covering the bone surfaces

The decalcified histological sections of cortical compacta and cancellous bone of the cat with hyperostosis, compared with the control cat, revealed marked differences in density and architecture. Cortical thickness of the affected cat measured 0.8 mm compared with 0.5 mm for the control cat. While the number of bony trabecular systems was reduced in the affected cat as compared with the control cat, bony trabeculae in the hyperostotic cat were stouter and had a haphazard arrangement that lacked the normal architectural pattern for cancellous bone seen in the control cat. Patchy areas of periosteal new bone deposition, and cortical and cancellous bone remodelling activity were present in the affected cat but absent in the control. Goldner's trichrome-stained bone specimens revealed wide, poorly mineralised bone deposits on bone surfaces in the affected cat (Figure 11).

In the cat with the hyperostotic skeleton, the resorption spaces in the cortical bone were increased as compared with the normal littermate. While the numbers of bony trabeculae of cancellous bone were reduced, the thickness of

the remaining bony trabeculae was increased. The normal architectural pattern of trabecular bone spanning the medullary cavity of the bones was absent in the hyperostotic cat. However, the adipose tissue and the thickness of bone lining cells in the affected cat were similar to those of the control cat (Figure 12). Bone density was in agreement with μCT.

TRAP-positive osteoclasts had an unremarkable histological appearance in both the affected and unaffected cats (Figure 13); however, increased numbers of osteoclasts were present in the affected cat (21/mm^2) as compared with the unaffected littermate (6.9/mm^2). This is compatible with increased bone remodelling activity.

Undecalcified sections were obtained only from the affected cat. Fluorescent labelling of active bone formation revealed numerous surfaces actively forming bone. The mineral apposition rate was calculated as being 1.38 µm/day. We did not have access to a labelled bone biopsy from an age-matched normal cat for comparison, nor could we locate such data in the published literature. In addition to assessing bone formation, we performed a Goldner's trichrome stain which demonstrates mineralising osteoid. The biopsy from the affected cat showed many sites of non-mineralised osteoid (Figure 11). This suggests elevated bone turnover in the affected cat. Although we did not have control bone to compare this with, such large amounts of active bone formation would not be expected in a mature cat.

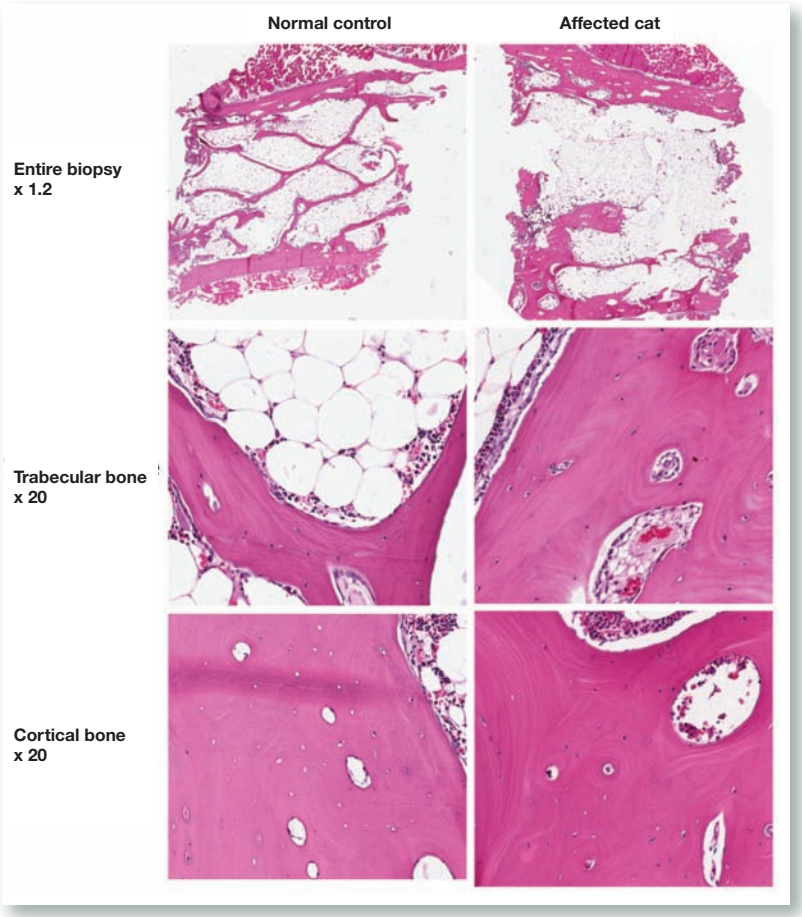

Figure 12 Haematoxylin and eosin stained decalcified bone sections from the affected and unaffected cats. Note extensive changes in the trabecular and cortical architecture. The marrow cells in the affected cat appear normal, but the trabecular bone appears corticalised when compared with the unaffected cat

Molecular genetics

Genomic DNA was isolated from whole blood from the affected cat and from an unrelated control cat. Using the UCSC cat genome assembly (felCat5), primers were designed to amplify the coding exons of SOST (chrE1:71795923-71808882) and adjacent intronic regions.

Amplicons were generated using Taq DNA Polymerase. Polymerase chain reaction (PCR) fragments were resolved on a 1% agarose gel and visualised with ethidium bromide. PCR products were treated with 1 U Shrimp Alkaline Phosphatase and 6 U Exonuclease I. All DNA sequencing was performed on a 3730xl capillary sequencer.

There were a number of heterozygous and homozygous changes identified in both the proband and control. Changes in SOST that were likely to be pathogenic were not found.

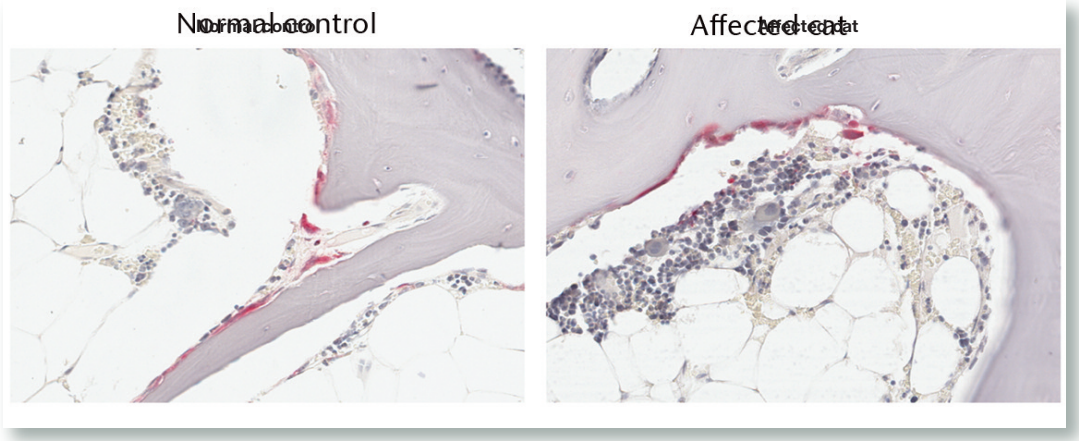

Figure 13 Representative sections from the unaffected and affected cats stained with TRAP for osteoclasts and counterstained with haematoxylin. Osteoclasts appear red; nuclei and bone matrix appear purple. Osteoclast morphology did not appear altered in the affected cat. Original magnification x 30

Discussion

Disorders that cause increased bone size in cats are uncommon. The maintenance of healthy bone depends on normal bone remodelling, with old bone being resorbed by osteoclasts and new bone formed by osteoblasts.[2] Abnormally increased bone density reflects an imbalance in bone turnover, which may be congenital or acquired.[2] Diagnostic possibilities for increased bone density in cats include osteopetrosis, FeLV-induced medullary osteosclerosis and secondary hypertrophic osteodystrophy (SHO).

Osteopetrosis refers to a well characterised bone disorder that causes increased bone density. Commonly it is an incidental finding and affected cats have increased medullary opacity[3] and endosteal thickening of the cortex.[2] In these two previous feline reports, the condition was characterised by an increase in bone mass due to cortical thickening and mineralisation within the medulla, without overall enlargement of affected bones.[2,3] In Wright et al's study, 10/11 affected cats died of an unrelated disease within 6 months of detection of radiographic signs of osteopetrosis, raising the possibility that the condition is secondary to concurrent disease.[3] A condition that is radiographically similar to osteopetrosis has been reported following experimental inoculation of kittens with FeLV.[4] Wright et al proposed that osteopetrosis be replaced by diffuse osteosclerosis when describing this disorder.[3]

We make the distinction between disorders that cause increased bone mass without overall increase in bone size (osteosclerosis), and disorders that cause increased bone mass and increased bone size (hyperostosis), and propose that the condition that we have encountered in this cat is an example of generalised hyperostosis. Based on the morphologic appearance of the bones of the cat in this report, it is unlikely that the bone changes were caused by osteopetrosis.

SHO, generally regarded as a paraneoplastic disorder (although not always the case), is characterised by bilaterally symmetrical subperiosteal new bone proliferation that affects the diaphyses of any long bones of the appendicular skeleton, especially distally. Radiographically it is recognised by irregular palisades of new bone proliferation that overlie relatively normal cortical bone. The medullary cavity is unaffected. Typically, it is bones of the extremities that appear to be first affected, so the paws become noticeably swollen. Bone enlargement progresses proximally, and can affect bones of the axial skeleton. At least 10 cases of feline SHO have been reported.[5] In all but one case,[6] the underlying pathology was determined and included thoracic and abdominal neoplasia and, in one instance, a tuberculous granuloma in the chest.

SHO is an unlikely cause for the condition reported here for several reasons. The radiographic appearance of new bone is not consistent with SHO, being homogeneous, smoothly marginated and appearing to seamlessly incorporate the cortex. Clinically the cat has remained stable during 4 years of observation. There is no radiographic evidence of progression of the bony changes, and thoracic radiography and abdominal ultrasonography have failed to detect signs of persistent concurrent disease. We presume that the transient radiographic lung lesion was inflammatory in origin as it resolved spontaneously, or secondarily to oxytetracycline administration.

Two other conditions that are worthy of consideration are hypervitaminosis A,[7] and Scottish Fold osteochondrodysplasia.[8] In both there is bony proliferation causing bone enlargement, but the anatomical location of proliferative changes is generally around the joints of the appendicular skeleton in the case of Scottish Fold osteochondrodysplasia, while, in hypervitaminosis A, bony proliferation causes ankylosing spondylopathy of the spine, sternum and elbows. The cat in this report did not have folded ears and was not fed a diet likely to induce hypervitaminosis A. Furthermore, the anatomical distribution of bone changes in this case is atypical for both Scottish Fold osteochondrodysplasia and hypervitaminosis A.

Regional hyperostosis is a feature of several conditions reported in dogs, but so far not replicated in domestic cats. Craniomandibular osteopathy affects the rami of the mandibles, the tympanic bullae and occasionally the long bones.[9] It is mostly seen in small dogs of terrier breeds, but has been reported in large dogs.[10] Its onset coincides with the period of bone formation in juveniles; it is often self-

We distintinguish between disorders that cause increased bone mass without overall increase in bone size (osteosclerosis), and disorders that cause increased bone mass and increased bone size (hyperostosis), and propose that the condition encountered in this cat is an example of generalised hyperostosis.

limiting, and may regress and disappear when bone growth is complete. There may be some crossover between craniomandibular osteopathy and another condition of dogs, metaphyseal osteopathy (formerly known as hypertrophic osteodystrophy).[11,12]

In metaphyseal osteopathy the primary radiographic lesion is in the metaphyses of long bones of juvenile dogs, where osteonecrosis causes an irregular radiolucent zone in the metaphysis roughly parallel to the growth plate. As the disorder progresses a collar of extraperiosteal new bone proliferation develops around the affected metaphysis, eventually becoming incorporated into the underlying periosteum. Affected animals also exhibit signs of dysfunction in other organs, due to a widespread immune-mediated vasculitis. In this respect, metaphyseal osteopathy is a truly polysystemic disorder, unlike craniomandibular osteopathy, but the proliferative metaphyseal changes and occasional bone proliferation on the rami of the mandibles can create a similar radiographic picture. Metaphyseal osteopathy causes affected animals to be painful and unwell, but after appropriate treatment with corticosteroids the condition resolves and bone formation returns to normal.

A third condition that produces regional hyperostosis is the calvarial hyperostosis syndrome.[13] This also affects juvenile dogs, to date limited to Bullmastiffs. Calvarial thickening involving the frontal, parietal and occipital bones is an important radiographic feature. Proliferative bone changes affecting the diaphyses of some bones of the appendicular skeleton also occur in some dogs. It has been suggested that osteomyelitis may occur concurrently with calvarial hyperostosis and some cases have been treated successfully with antibiotics.

In lions (*Panthera leo*) calvarial hyperostosis has been linked to hypovitaminosis A,[14] a condition where hyperostosis of the occipital bone compresses the foramen magnum. The atlas is also thickened.

In the human literature, several disorders present as diaphyseal hyperostosis and bear some radiographic resemblance to this case; namely, hyperostosis corticalis generalisata (Van Buchem disease),[15,16] Camurati–Engelmann disease (progressive diaphyseal dysplasia)[17] and melorheostosis.[15]

In Van Buchem disease there is hyperostosis of the diaphyses of the long bones, mandible, calvarium, ribs and clavicles.[18] The disease is described as being characterised by endosteal hyperostosis. Radiographically, affected bones are thickened; in particular, the mandibles are impressively enlarged. The disease is inherited as an autosomal recessive trait. Bone growth is continuous throughout life, and it has been postulated (but unproven) that the underlying mechanism is increased osteoblastic activity.

Camurati–Engelmann disease has morphological radiographic features of skull, pelvic and long bone hyperostosis.[17] Typically the long bone changes affect the diaphyses without metaphyseal or epiphyseal involvement. The joints of the appendicular skeleton appear normal. Unlike Van Buchem disease, the mandible is spared. Camurati–Engelmann disease is an autosomal dominant disorder characterised by a molecular defect in the gene encoding transforming growth factor beta-1.[19] Affected individuals often have painful extremities and fatigue easily.

Melorheostosis is a mesenchymal disease that affects the skeleton and adjacent soft tissues.[20] Its pathogenesis is unclear and it is generally believed not to be inherited. Affected individuals usually show extensive bone involvement. The flowing hyperostosis or 'dripping candlewax' pattern described as characteristic of melorheostosis is not always present. Bone changes are not distributed symmetrically and may affect only one bone or bones of one limb.[21] Patterns of hyperostosis are variable, including osteoma-like, cortical thickening and 'dripping candlewax'. In addition, soft tissue mineralisation such as myositis ossificans may be present.

In the affected cat in this report the increased urea concentration may be due to muscle catabolism, although a renal component cannot be ruled out on account of the low urine specific gravity and history of recurrent urinary tract infections.

Currently, we are unable to determine a single mechanism or combination of mechanisms responsible for the bony abnormalities in this patient, but we anticipate a genetic basis.

Currently, we are unable to determine a single mechanism or combination of mechanisms responsible for the bony abnormalities in this cat, but we anticipate a genetic basis.

Conclusions

Disorders that cause bone sclerosis may be divided into those causing increased bone density without modification of bone shape, such as osteopetrosis, and those that cause increased bone density with modification of shape, such as metaphyseal osteopathy. In this report we describe a third subtype, a cat with increased bone density and modification of the size and shape of the osseous skeleton. By convention, osteosclerosis refers to trabecular bone thickening, and hyperostosis to cortical bone thickening. Because the affected cat had demonstrable cortical thickening we name the syndrome hyperostosis. Although we have anecdotal reports of several other similar examples of feline generalised hyperostosis, this condition has not previously been reported in cats.

Acknowledgements

The authors would like to acknowledge the invaluable assistance of Dr Leigh Waddell, Laboratory and Diagnostics Manager for the Institute for Neuroscience and Muscle Research, NSW, Australia, for assistance in performing the DNA analysis.

Funding

The authors received no specific grant from any funding agency in the public, commercial or not-for-profit sectors for the preparation of this report.

Conflict of interest

The authors do not have any potential conflicts of interest to declare.

References

1 Gruber HE, Ingram J and Hanley EN Jr. **An improved staining method for intervertebral disc tissue.** *Biochem Histochem* 2002; 77: 81–83.
2 Kramers P, Fluckiger MA, Rahn BA and Cordey J. **Osteopetrosis in cats.** *J Small Anim Pract* 1988; 29: 153–164.
3 Wright MW, Hudson JA and Hathcock JT. **Osteopetrosis in cats: clarification of a common misnomer** [Abstract]. Scientific Meeting of the American College of Veterinary Radiologists; 2002 Dec 3–7; Chicago, Illinois. *Vet Radiol Ultrasound* 2003; 44: 106.
4 Hoover EA and Kociba GJ. **Bone lesions in cats with anemia induced by feline leukemia virus.** *J Natl Cancer Inst* 1974; 53: 1277–1284.
5 Foster SF. **Idiopathic hypertrophic osteopathy in a cat.** *J Feline Med Surg* 2007; 9: 172–173.
6 Ocarino ND, Fukushima FB, Gomes AD, Bueno DF, de Oliveira TS and Serakides R. **Idiopathic hypertrophic osteopathy in a cat.** *J Feline Med Surg* 2006; 8: 345–348.
7 Seawright AA, English PB and Gartner RJW. **Hypervitaminosis A and hyperostosis of the cat.** *Nature* 1965; 206: 1171–1172.
8 Malik R, Allan GS, Howlett CR, Thompson DE, James G, McWhirter C, et al. **Osteochondrodysplasia in Scottish Fold cats.** *Aust Vet J* 1999; 77: 85–92.
9 Riser WH, Parkes LJ and Shirer JF. **Canine craniomandibular osteopathy.** *J Am Vet Radiol Soc* 1967; 8: 23–31.
10 Watson ADJ, Huxtable CR and Farrow BRH. **Craniomandibular osteopathy in Doberman Pinschers.** *J Small Anim Pract* 1975; 16: 11–19.
11 Woodard JC. **Canine hypertrophic osteodystrophy, a study of the spontaneous disease in littermates.** *Vet Pathol* 1982; 19: 337–354.
12 Rendano VT, Dueland R and Sifferman RL. **Metaphyseal osteopathy – (hypertrophic osteodystrophy).** *J Small Anim Pract* 1977; 18: 679–683.
13 McConnell JF, Hayes A, Platt SR and Smith KC. **Calvarial hyperostosis syndrome in two bullmastiffs.** *Vet Radiol Ultrasound* 2006; 47: 72–77.
14 Gross-Tsubery R, Chai O, Shilo Y, Miara L, Horowitz IH, Shmueli A, et al. **Computed tomographic analysis of calvarial hyperostosis in captive lions.** *Vet Radiol Ultrasound* 2010; 51: 34–38.
15 Vanhoenacker FM, De Beuckeleer LH, Van Hul W, Balemans W, Tan GJ, Hill SC, et al. **Sclerosing bone dysplasias: genetic and radioclinical features.** *Eur Radiol* 2000; 10: 1423–1433.
16 van Lierop AH, Hamdy NAT, van Egmond ME, Bakker E, Dikkers FG and Papapoulos SE. **Van Buchem disease: clinical, biochemical, and densitometric features of patients and disease carriers.** *J Bone Miner Res* 2013; 28: 848–854.
17 Vanhoenacker FM, Janssens K, Van Hul W, Gershoni-Baruch R, Brik R and De Schepper AM. **Camurati–Engelmann disease – review of radioclinical features.** *Acta Radiol* 2003; 44: 430–434.
18 Van Hul W, Balemans W, Van Hul E, Dikkers FG, Obee H, Stokroos RJ, et al. **Van Buchem disease (hyperostosis corticalis generalisata) maps to chromosome 17q12-q21.** *Am J Hum Genet* 1998; 62: 391–399.
19 Janssens K, Vanhoenacker F, Bonduelle M, Verbruggen L, Van Maldergem L, Ralston S, et al. **Camurati-Engelmann disease: review of the clinical, radiological, and molecular data of 24 families and implications for diagnosis and treatment.** *J Med Genet* 2006; 43: 1–11.
20 Freyschmidt J. **Melorheostosis: a review of 23 cases.** *Eur Radiol* 2001; 11: 474–479.
21 Suresh S, Muthukumar T and Saifuddin A. **Classical and unusual imaging appearances of melorheostosis.** *Clin Radiol* 2010; 65: 593–600.